

Effect of Symmetry on Insertion Loss in SRR and CSRR Transmitarray Unit Cells Implementing the Element Rotation Method

Emre Erdil¹, Kagan Topalli², and Ozlem Aydin Civi¹

¹Department of Electrical and Electronics Engineering
Middle East Technical University, Ankara, Turkey
eerdil@gmail.com, ozlem@metu.edu.tr

²TUBITAK Space Technologies Research Institute
Microwave and Antenna Systems Group, Ankara, Turkey
kagan.topalli@tubitak.gov.tr

Abstract — Insertion loss variation with respect to rotation angle is examined for geometrically symmetrical and unsymmetrical split ring resonators (SRR) and complementary split ring resonators (CSRR) transmitarray unit cells implementing the element rotation method. Generalized design conditions for the implementation of the method on transmitarrays are derived. Based on the S-parameters obtained by full-wave electromagnetic simulations and field analysis, it is shown that the symmetry of CSRR unit cells has an important effect on decreasing insertion loss variation with respect to rotation angle. Up to 3 dB improvement in insertion loss is achieved for the symmetrical single ring double split CSRR type unit cell. It is also shown for two nested non symmetric SRR unit cells that, insertion loss is almost independent of the element rotation when the transmission is mainly provided by the symmetrical part of the unit cell.

Index Terms — CSRR, element rotation method, SRR, transmitarray.

I. INTRODUCTION

The element rotation method is used to control the phase of the waves scattered from the structures excited by circularly polarized electromagnetic waves in reflectarrays and transmitarrays. The conditions for element rotation required to achieve phase shifting are derived for reflectarrays [1], [2] and transmitarrays [3]. The element rotation method is employed in several antennas [1]-[13]. The conditions for transmitarrays [3] cover symmetrical structures with respect to all orthogonal planes. In this letter, the generalized conditions are derived without being restricted by symmetry.

Since the design of a transmitarray is implemented through the analysis of a unit cell, it is crucial to analyze the parameters that may affect the overall characteristics

of the transmitarray at the unit cell level. Insertion loss is a parameter that has an influence on the gain and efficiency of a transmitarray. Therefore, besides analyzing the insertion loss of a unit cell and its variation with respect to rotation angle, it is also important to determine the factors affecting insertion loss and to propose a solution to alleviate the variations of insertion loss.

To the author's knowledge, although variations of reflection and transmission magnitude with respect to rotation angle are presented in the literature, the reasons of these variations are not clarified [3]. Therefore, to understand the physics behind these amplitude variations with rotating angle, this work focuses on the sources of insertion loss variations with respect to rotation angle in a group of SRR and CSRR type transmitarray unit cells employing the element rotation method. The investigation by full wave EM simulations is found to be sufficient, as the simulations provide a controlled environment and eliminate some other effects that might arise in manufacturing and measurement. It is shown by simulations that, for the presented structures, insertion loss variation depends on the axial symmetry of the element and symmetry has an effect on decreasing the value of the variation.

II. GENERALIZED DESIGN CONDITIONS AND MAGNITUDE VARIATION IN THE ELEMENT ROTATION METHOD

In this section, the conditions that should be satisfied by the unit cells to implement the element rotation method are derived in the most general sense. The transmission magnitude on the derived circularly-polarized S-parameters is investigated.

The most practical method of obtaining the phase design curve of a unit cell is the infinite array approach. In this approach, the array is formed by replicating identical unit cells. The approach provides an opportunity for designing array structures by analyzing only a single

element, i.e., unit cell with periodic boundary conditions, including the effect of mutual coupling between the elements. Infinite array approach is implemented using Finite Element Method (FEM) solver of Ansys HFSS®. In HFSS®, in order to satisfy this periodicity, periodic boundary conditions are implemented by master and slave boundaries on the unit cell walls. The E-field in any point of the slave boundary matches the correspondent point of the master boundary with a phase difference [14]. The periodic arrangement of the array allows the approximation of the infinite array fields with Floquet modal expansion. Floquet ports are defined on the apertures of the unit cell as an interface to unbounded medium and the fields on the ports are represented by a set of Floquet modes. A Floquet mode is a plane wave function and these modes define the discrete directions where an infinite array radiates plane waves. The number of the propagating modes is related to the dimensions of the unit cell and the incidence angle. The dominant mode corresponds to the main beam of the antenna whereas higher order modes correspond to the grating lobes and when the unit size is less than half a wavelength, only the dominant mode propagates [3]. The propagating modes can be decomposed into orthogonal modal functions, TE and TM, for simplicity. This normalization is useful in layered structures as these orthogonal modal functions propagate without producing the other transverse mode for homogeneous and isotropic media. That is, TE (TM) mode will not produce a TM (TE) mode [15]. Therefore, for a unit cell smaller than half a wavelength the propagating dominant mode is decomposed into one TE and one TM propagating modes and individual analysis of these modes are performed by using HFSS®. In the infinite array approach since the analysis is carried out by using a single unit cell, the computation time and the utilization of the computational resources are reduced. However, in this approach, infinite extension of the unit cell causes ignoring of the edge effects and the mutual coupling only includes the coupling between identical elements. These conditions may affect the phase response of the structure. Different approaches taking into account the coupling of non-identical cells are implemented to make a comparison with the infinite array approach in [16]. The infinite array approach is widely used in large array structures and it provides results in very good agreement with measurements by offering a very fast computation.

In the simulations of this study, only the dominant Floquet mode incidence is considered and it is decomposed as x - and y -polarized wave modes for a plane wave propagating along the z -axis [3].

The relation between the incident, a , and scattered, b , wave modes can be written in terms of S-parameters as,

$$\begin{bmatrix} b_1^x \\ b_1^y \\ b_2^x \\ b_2^y \end{bmatrix} = \begin{bmatrix} s_{11}^{xx} & s_{11}^{xy} & s_{12}^{xx} & s_{12}^{xy} \\ s_{11}^{yx} & s_{11}^{yy} & s_{12}^{yx} & s_{12}^{yy} \\ s_{21}^{xx} & s_{21}^{xy} & s_{22}^{xx} & s_{22}^{xy} \\ s_{21}^{yx} & s_{21}^{yy} & s_{22}^{yx} & s_{22}^{yy} \end{bmatrix} \begin{bmatrix} a_1^x \\ a_1^y \\ a_2^x \\ a_2^y \end{bmatrix}, \quad (1)$$

where the subscripts and superscripts of a and b represent the number of the Floquet port and the direction of polarization, respectively. Following the same procedure in [3], circularly polarized S-parameters are obtained in terms of linearly polarized ones and are given as,

$$s_{11}^{rl} = \frac{1}{2} \left[\left(s_{11}^{xx} + s_{11}^{yy} \right) - j \left(s_{11}^{xy} - s_{11}^{yx} \right) \right], \quad (2-3)$$

$$s_{11}^{ll} = \frac{1}{2} \left[\left(s_{11}^{xx} - s_{11}^{yy} \right) e^{-j2\psi} + j \left(s_{11}^{xy} + s_{11}^{yx} \right) e^{+j2\psi} \right], \quad (4-5)$$

$$s_{12}^{ll} = \frac{1}{2} \left[\left(s_{12}^{xx} + s_{12}^{yy} \right) - j \left(s_{12}^{xy} - s_{12}^{yx} \right) \right], \quad (6-7)$$

$$s_{12}^{rl} = \frac{1}{2} \left[\left(s_{12}^{xx} - s_{12}^{yy} \right) e^{-j2\psi} + j \left(s_{12}^{xy} + s_{12}^{yx} \right) e^{+j2\psi} \right], \quad (8-9)$$

$$s_{21}^{ll} = \frac{1}{2} \left[\left(s_{21}^{xx} + s_{21}^{yy} \right) - j \left(s_{21}^{xy} - s_{21}^{yx} \right) \right], \quad (10-11)$$

$$s_{21}^{lr} = \frac{1}{2} \left[\left(s_{21}^{xx} - s_{21}^{yy} \right) e^{-j2\psi} + j \left(s_{21}^{xy} + s_{21}^{yx} \right) e^{+j2\psi} \right], \quad (12-13)$$

$$s_{22}^{rl} = \frac{1}{2} \left[\left(s_{22}^{xx} + s_{22}^{yy} \right) - j \left(s_{22}^{xy} - s_{22}^{yx} \right) \right], \quad (14-15)$$

$$s_{22}^{rr} = \frac{1}{2} \left[\left(s_{22}^{xx} - s_{22}^{yy} \right) e^{-j2\psi} + j \left(s_{22}^{xy} + s_{22}^{yx} \right) e^{+j2\psi} \right], \quad (16-17)$$

where the superscripts l and r denote the sense of the polarization, i.e., left hand and right hand, respectively whereas ψ denotes the rotation angle. For the equations above, each line includes two separate equations where the first one is given by the upper superscripts.

In a transmitarray design, minimization of reflection is an important design consideration to increase the antenna efficiency. For an efficient transmitarray unit cell design, all the reflections should be minimized as,

$$s_{11}^{xx} = s_{11}^{yy} = s_{22}^{xx} = s_{22}^{yy} = s_{11}^{xy} = s_{11}^{yx} = s_{22}^{xy} = s_{22}^{yx} = 0. \quad (18)$$

It is seen from the equations that for each sense of polarization, two transmission parameters exist i.e., when we illuminate the structure by a left-hand circularly polarized wave from port 1, left and right-hand circularly polarized transmissions, s_{21}^{ll} and s_{21}^{rl} , take place. The transmission with the same sense of polarization is not affected from rotation and forms cross-pol radiation. To eliminate the scattered transmission fields independent of rotation, following conditions should be satisfied in the design,

$$s_{mn}^{xx} = -s_{mn}^{yy}, \quad (19)$$

$$s_{mn}^{xy} = s_{mn}^{yx} \text{ for } m, n = 1, 2 \text{ and } m \neq n. \quad (20)$$

Satisfying these, four parameters are left; (8), (9), (12), and (13). Two of these parameters, (9) and (13) are advancing the transmitted phase twice the rotation angle, whereas (8) and (12) are delaying it. Also, the sense of

polarization changes for the transmitted wave.

(18)–(20) together with the maximization of transmission are the general conditions for applying the element rotation method in the transmitarrays. Although the implementation of (20) requires no phase difference between s_{mn}^{xy} and s_{mn}^{yx} , minimizing these components also reduces the cross-pol radiation even if there is a phase difference between them.

Further simplification is also possible for symmetrical structures with respect to the xy -plane. If we define, s_{21}^{xx} and s_{12}^{xx} as T_x ; s_{21}^{yy} and s_{12}^{yy} as T_y ; s_{21}^{xy} and s_{12}^{xy} as T_{xy} ; s_{21}^{yx} and s_{12}^{yx} as T_{yx} for a symmetrical structure with respect to xy -plane; minimizing reflection, maximizing T_x and T_y and having 180° of phase difference between them when they have equal magnitude as implied by (19) and having 0° of phase difference between T_{xy} and T_{yx} when they have equal magnitude as implied by (20) or minimizing them are the sufficient conditions to design a transmitarray employing element rotation method.

The circularly polarized transmission parameters after satisfying conditions, (8), (9), (12), and (13) demonstrate that the phase of the transmitted wave changes twice the rotation angle without changing the magnitude. However, full-wave EM simulations indicate that the magnitude changes with the change in the rotation angle. This is mainly because the amount of the existing electromagnetic coupling between the elements changes with the rotation angle [2]. Since this coupling affects overall array characteristics [4], it is important to determine the parameters reducing the adverse effects of it on insertion loss. It should also be noted here that the element rotation method assumes the rotation of the entire structure with its environment including the lattice, around its surface normal [3]. However, in an array, the edges of the unit cell generate a boundary that does not rotate with the rotation of the array element. Therefore, even if all the components of the radiators inside the unit cell rotate, the array and the unit cell boundaries are stationary which has an effect on the magnitude of transmitted and reflected fields.

A. CSRR designs

Figures 1 (a)–(d) show the schematics and the transmission magnitudes of the examined CSRR unit cells which are, nested CSRR (N-CSRR), single ring double split CSRR (DS-CSRR), and single ring single split CSRR (SS-CSRR). All the structures satisfy the conditions for shifting the phase linearly with respect to rotation angle at the operating frequency. The size of the unit cells is $10.16 \text{ mm} \times 10.16 \text{ mm}$, the substrate is glass, ($\epsilon_r=4.6$, $\tan \delta=0.005$), having a thickness of 6 mm and the operating frequency is 9.9 GHz in all structures. The dimensions of the structures are given in Table 1. From transmission magnitudes of the unit cells, it is realized that transmission

behaviors of the structures are similar and the magnitude varies with the change in rotation angle. Insertion loss is less for the symmetrical structure, DS-CSRR.

To extract the relationship between symmetrical geometry and insertion loss level, insertion loss levels of DS-CSRR and SS-CSRR structures are examined. Ideal cases are constructed by evaluating linearly polarized S-parameters at $\psi = 0^\circ$ from simulations and then taking the rotation angle (ψ) into account using equation (12). In Fig. 1 (e), insertion loss values as a function of rotation angle directly obtained from full wave simulations are compared with the values of ideal cases. It is observed that insertion loss calculated through full wave simulations of DS-CSRR is more similar to insertion loss obtained by applying (12) on DS-CSRR. The reason why the variation of insertion loss of the symmetrical structure (DS-CSRR) is smaller compared to that of the unsymmetrical structure (SS-CSRR) is not evident from analytical expressions, since the values of the linearly polarized S-parameters do not change when the structure is rotated. This is investigated in the following sections by analyzing fields and currents.

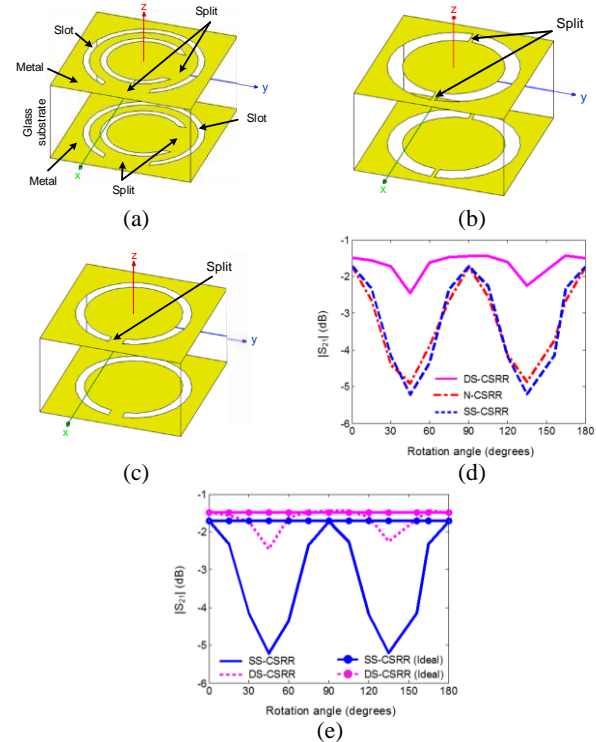


Fig. 1. CSRR unit cells: (a) N-CSRR, (b) DS-CSRR, (c) SS-CSRR, (d) circularly polarized transmission coefficients of the CSRR unit cells with respect to the rotation angle, and (e) circularly polarized transmission coefficients of DS-CSRR and SS-CSRR unit cells with respect to rotation angle and compared to their ideal cases.

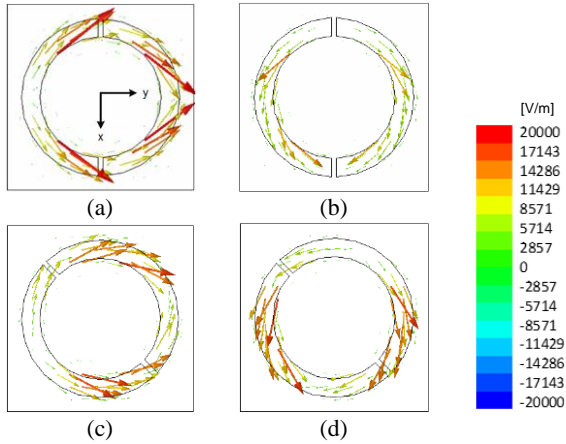


Fig. 2. Magnetic surface current density distributions for the DS-CSRR: (a) for x -polarized wave modes at 0° , (b) for y -polarized wave modes at 0° , (c) for x -polarized wave modes at 45° , and (d) for y -polarized wave modes at 45° .

Table 1: Dimensions of the CSRR unit cells

	SS-CSRR	DS-CSRR	N-CSRR
Split length (mm)	1	0.26	3.3 (both splits)
Ring slot width (mm)	4 – 3.38	4.3 – 3.3	4.2 – 3.75 (outer ring) 3 – 2.55 (inner ring)

B. Field analysis of CSRR designs

A field analysis is carried out on the designs to show the relation between the symmetry and the variation of insertion loss. Magnetic surface current density distributions (tangential electric field on the slot), M_s , on the ring slots of the DS-CSRR obtained for x - and y -polarized incident waves at 9.9 GHz are plotted in Fig. 2. It is observed that the symmetrical distribution of M_s is not affected by rotation for both polarizations. Figure 3 depicts M_s for the SS-CSRR. At $\psi = 45^\circ$, the distribution is significantly denser at one arm of the ring which increases the cross-polarized radiation. Comparing Fig. 2 and Fig. 3, it is seen that the symmetry of M_s is more distorted by rotation for the SS-CSRR compared to the DS-CSRR. This increases the cross-polarized terms in the S -parameters and cross-polarized radiation, which in turn affect the transmission characteristics of the element.

C. SRR designs

Figures 4 (a) and (b) show the SRR schematics. There is a single split on each design which disturbs the symmetrical geometry. The split takes place on the inner ring for one design whereas it takes place on the outer ring for the other design. These are called inner split SRR (IS-SRR) and outer split SRR (OS-SRR), respectively. As in the CSRR designs, the conditions for linear phase shifting are satisfied at 9.9 GHz for the substrate thickness of

6 mm. Other parameters of the structures are given in Table 2. It is observed from Fig. 4 (c) that, although both structures are unsymmetrical for the same plane, IS-SRR has much less insertion loss variation with the rotation angle.

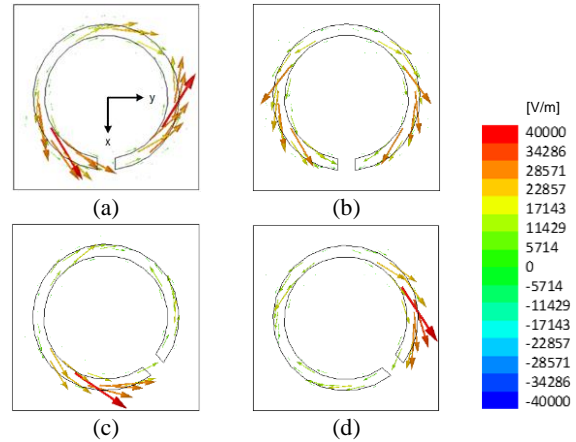


Fig. 3. Magnetic surface current density distributions for the SS-CSRR: (a) for x -polarized wave modes at 0° , (b) for y -polarized wave modes at 0° , (c) for x -polarized wave modes at 45° , and (d) for y -polarized wave modes at 45° .

Table 2: Dimensions of the SRR unit cells

	IS-SRR	OS-SRR
Split length (mm)	1.2	1.2
Ring width (mm)	4.29 – 3.49 (outer ring) 3.17 – 2.37 (inner ring)	3.95 – 3.45 (outer ring) 1.7 – 1.2 (inner ring)

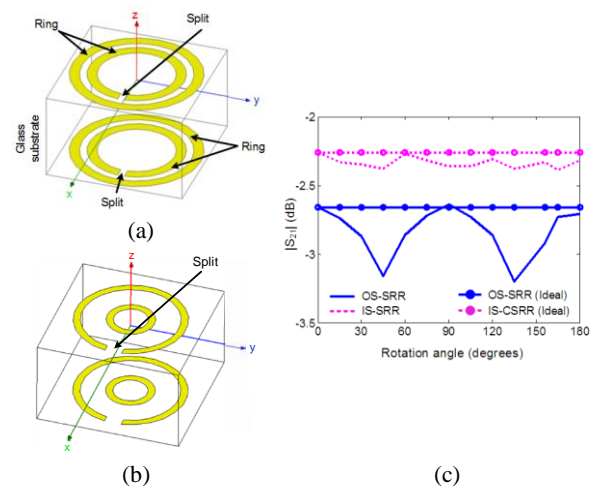


Fig. 4. (a) The inner split SRR (IS-SRR), (b) the outer split SRR (OS-SRR), and (c) circularly polarized transmission coefficient of the SRR unit cells.

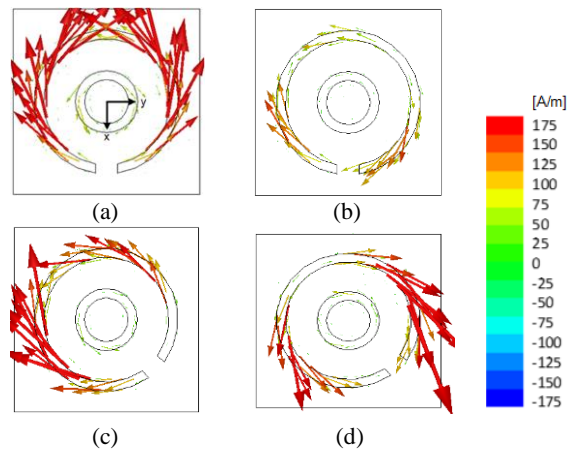


Fig. 5. Electric surface current density distributions for the OS-SRR: (a) for x -polarized wave modes at 0° , (b) for y -polarized wave modes at 0° , (c) for x -polarized wave modes at 45° , and (d) for y -polarized wave modes at 45° .

The J_s diagrams for OS-SRR, in Fig. 5, show that for both polarizations the resonance is mainly determined from the outer ring due to a strong current flow on that ring. Therefore, the disturbance on the current distribution on the outer ring affects the radiation and the transmission magnitude. When the OS-SRR is rotated to $\psi = 45^\circ$, it is seen in Figs. 5 (c) and (d) that the cross-polarized radiation increases which in turn increases the insertion loss. When the J_s diagrams for IS-SRR in Figs. 6 (a) and (b) are examined, it is observed that for x -polarized excitation, the outer ring and the inner ring generate the resonance together whereas for y -polarized excitation, the resonance is mainly determined from the outer ring due to a stronger current flow on that ring. As the rings get closer to each other, the coupling between them is stronger. When the rings are rotated, the symmetrical distribution on the inner ring is distorted which in turn affects the distribution on the outer ring due to coupling. This situation is less pronounced for y -polarized excitation as the outer ring is dominant on the determination of the resonance for that polarization. Therefore, the current distributions over the rings are more uniform for y -polarization which result in less insertion loss variation. Smaller variation of insertion loss for IS-SRR is mainly due to two reasons: (i) the outer ring where the current distribution is denser for one of the polarizations does not have a split, i.e., the outer ring is symmetrical to the orthogonal planes, and (ii) the split is closer to the center of the unit cell which results in lower coupling levels among adjacent cells when the unit cell is rotated.

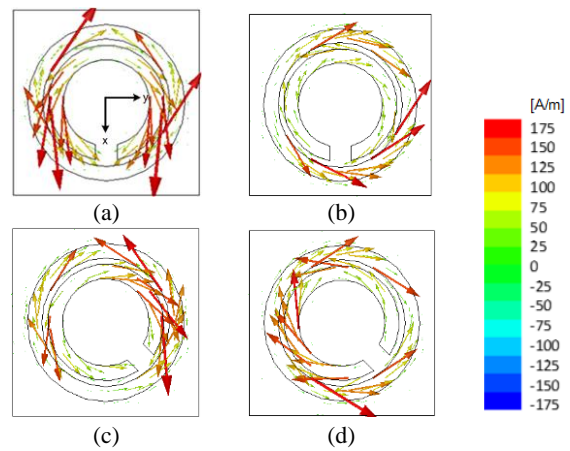


Fig. 6. Electric surface current density distributions for the IS-SRR: (a) for x -polarized wave modes at 0° , (b) for y -polarized wave modes at 0° , (c) for x -polarized wave modes at 45° , and (d) for y -polarized wave modes at 45° .

III. CONCLUSION

The effect of symmetrical geometry on insertion loss of CSRR and SRR-based transmitarray unit cells is demonstrated. The symmetrical geometry decreases cross-polarized scattering, which in turn decreases insertion loss variation with respect to rotation. It is also shown for unsymmetrical SRR structures that if the resonance is mainly provided by the symmetrical part of a unit cell, element rotation does not adversely affect the insertion loss. This work proposes a methodology to increase the transmission magnitude for SRR and CSRR-based transmitarray unit cells and is useful in understanding of the sources of the degradation of the radiation characteristics of transmitarrays.

ACKNOWLEDGMENT

This work was supported in part by TUBITAK, Project No. 113R033.

REFERENCES

- [1] J. Huang and R. J. Pogorzelski, "A Ka-band microstrip reflectarray with elements having variable rotation angles," *IEEE Trans. Antennas Propag.*, vol. 46, no. 5, pp. 650-656, May 1998.
- [2] C. Guclu, J. Perruisseau-Carrier, and O. Aydin Civi, "Proof of concept of a dual-band circularly-polarized RF MEMS beam-switching reflectarray," *IEEE Trans. Antennas Propag.*, vol. 60, no. 11, pp. 5451-5455, Nov. 2012.
- [3] R. H. Phillion and M. Okoniewski, "Lenses for

- circular polarization using planar arrays of rotated passive elements," *IEEE Trans. Antennas Propag.*, vol. 59, no. 4, pp. 1217-1227, Apr. 2011.
- [4] A. E. Martynyuk, J. I. Martinez Lopez, and N. A. Martynyuk, "Spiraphase-type reflectarrays based on loaded ring slot resonators," *IEEE Trans. Antennas Propag.*, vol. 52, no. 1, pp. 142-153, 2004.
- [5] B. Strassner, C. Han, and K. Chang, "Circularly polarized reflectarray with microstrip ring elements having variable rotation angles," *IEEE Trans. Antennas Propag.*, vol. 52, pp. 1122-1125, Apr. 2004.
- [6] M. Euler and V. F. Fusco, "Frequency selective surface using nested split ring slot elements as a lens with mechanically reconfigurable beam steering capability," *IEEE Trans. Antennas Propag.*, vol. 58, no. 10, pp. 3417-3421, Oct. 2010.
- [7] T. Smith, U. Gothelf, O.S. Kim, and O. Breinbjerg, "Design, manufacturing, and testing of a 20/30-GHz dual-band circularly polarized reflectarray antenna," *IEEE Antennas and Wireless Propagation Letters*, vol. 12, pp. 1480-1483, 2013.
- [8] M.-Y. Zhao, G.-Q. Zhang, X. Lei, J.-M. Wu, and J.-Y. Shang, "Design of new single-layer multiple-resonance broadband circularly polarized reflectarrays," *IEEE Antennas and Wireless Propagation Letters*, vol. 12, pp. 356-359, 2013.
- [9] S. Zainud-Deen, S. Gaber, H. Malhat, and K. Awadalla, "Single feed dual-polarization dual-band transmitarray for satellite applications," *ACES Journal*, vol. 29, no. 2, Feb. 2014.
- [10] E. Erdil, K. Topalli, N. S. Esmailzad, O. Zorlu, H. Kulah, and O. A. Civi, "Reconfigurable nested ring-split ring transmitarray unit cell employing the element rotation method by microfluidics," *IEEE Trans. Antennas Propag.*, vol. 63, no. 3, pp. 1163-1167, Mar. 2015.
- [11] S. Zainud-Deen, S. Gaber, H. Malhat, and K. Awadalla, "Single feed dual-polarization dual-band transmitarray for satellite applications," *ACES Journal*, vol. 29, no. 2, 2014.
- [12] S. H. Zainud-Deen, W. M. Hassan, and H. A. Malhat, "Near-field focused folded transmitarray antenna for medical applications," *ACES Journal*, vol. 31, no. 3, 2016.
- [13] A. Hassan, F. Yang, A. Z. Elsherbeni, and P. Nayeri, *Analysis and Design of Transmitarray Antennas*. Morgan and Claypool, 2017.
- [14] ANSYS® HFSS, Version 13, Online Help, Master and Slave Boundaries.
- [15] A. K. Bhattacharyya, *Phased Array Antennas: Floquet Analysis, Synthesis, BFNs, and Active Array Systems*. Hoboken, NJ: Wiley, 2006.
- [16] M-A. Milon, R. Gillard, D. Cadoret, and H. Legay, "Comparison between the "infinite array approach" and the "surrounded-element approach" for the

simulation of reflectarray antennas," *2006 IEEE Antennas and Propagation Society International Symposium*, Albuquerque, NM, pp. 4339-4342, 2006.



Emre Erdil was born in 1979. He received B.Sc., M.Sc. and Ph.D. degrees in Electrical and Electronics Engineering from Middle East Technical University (METU), Ankara, Turkey, in 2001, 2005, and 2007, respectively. Since 2002, he has been working at Capital Markets Board of Turkey. Erdil's recent research interests include reconfigurable transmitarrays and reflectarrays. He has also conducted research on MEMS-based reconfigurable antennas. Erdil is the recipient of "METU Thesis of the Year Award" in 2015.



Kagan Topalli was born in 1979. He received B.Sc. and Ph.D. degrees in Electrical and Electronics Engineering from Middle East Technical University (METU), Ankara, Turkey, in 2001 and 2007, respectively. Between 2001 and 2007, he has worked as a Research Assistant at METU in the Department of Electrical and Electronics Engineering. Between 2007 and 2010, he has worked as a Research Engineer at the METU-MEMS (MicroElectroMechanical Systems) Center. Topalli worked as a Post-doctoral Researcher at ElectroScience Laboratory of the Ohio State University between February 2010 and February 2012. He worked as a Faculty at TED University, Department of Electrical and Electronics Engineering in Ankara, Turkey. Topalli worked as a faculty at Bilkent University, National Nanotechnology Research Center (UNAM), Institute of Materials Science and Nanotechnology. He is currently working as a Chief Research Scientist at TUBITAK-Space Technologies Research Institute. Topalli's recent research interests include THz sensors and THz imaging systems. He has also conducted research on the development, characterization, and integration of novel RF MEMS structures for RF front ends at microwave and millimeter-wave, reconfigurable antennas, phased arrays, microwave packaging, and microfabrication technologies. He has published more than 60 journal and international conference papers. Topalli received the "METU Thesis of the Year Award" in 2007 for his Ph.D. dissertation, which was awarded by the Prof. Mustafa N. Parlar Education and Research Foundation. He received the "URSI (Union of Radio Science-International)

Young Scientist Award” in 2011. He received “Research Incentive Award” in 2013 given by the Prof. Mustafa N. Parlar Education and Research Foundation. He is the co-advisor to the recipient of “METU Thesis of the Year Award” in 2015. He is a Senior Member of IEEE.



Özlem Aydın Civi received B.Sc., M.Sc. and Ph.D. degrees in 1990, 1992 and 1996 respectively in Electrical and Electronics Eng. Department of the Middle East Technical University (METU) in Ankara, Turkey. She was a Research Assistant in METU between 1990-1996. In 1997-1998 she was a Visiting Scientist at the ElectroScience Laboratory, Ohio State University. Since 1998, she has been with the Department of Electrical and Electronics Engineering, METU, where she is currently

a Professor. Her research interests include analytical, numerical and hybrid techniques in EMT problems, especially fast asymptotic/hybrid techniques for the analysis of large finite periodic structures, multi-function antenna design, reconfigurable antennas, phased arrays, reflectarrays and RF-MEMS applications. She has published more than hundred and fifty journal and international conference papers. She was a recipient of 1994 Prof. Mustafa Parlar Foundation Research and Encouragement Award with METU Radar Group and 1996 URSI Young Scientist Award. She was the Chair of IEEE Turkey Section in 2006 and 2007, the Chair of IEEE AP/MTT/ED/EMC Chapter between 2004 and 2006. She is Vice Chair of the Turkish National Committee of URSI. She was an Associate Editor of the IEEE Transaction on Antennas and Propagation between 2010-2016.